Tribol Lett (2011) 41:425–434
DOI 10.1007/s11249-010-9728-8

ORIGINAL PAPER

# Hydrothermal Synthesis, Characterization, and Tribological Behavior of Oleic Acid-Capped Lanthanum Borate with Different Morphologies

**Zhengfeng Jia · Yanqiu Xia**

Received: 27 November 2009 / Accepted: 8 November 2010 / Published online: 18 November 2010


**Abstract** In this paper, nano/microstructure lanthanum borates were synthesized by hydrothermal route. Furthermore, oleic acid-capped nano/microstructure lanthanum borates (OANLBs) were also prepared. The nano/microstructure of lanthanum borate is characterized by means of Fourier transform-infrared spectroscopy (FT-IR), field-emission scanning electron microscopy (FE-SEM), and transmission electron microscopy (TEM). At the same time, the friction and wear properties of OANLBs as additives in poly-alpha-olefin (PAO) were measured for AISI 1045 steel and laser treated AISI 1045 steel. Results show that the PAO containing OANLBs possesses much better tribological properties for steel/steel and steel/laser treated AISI 1045 steel sliding pairs than pure PAO.

**Keywords** Nanoparticles · Lanthanum borate · Friction · Wear · XPS

## 1 Introduction

During the last decade, interest in the synthesis and properties of borate materials has steadily grown because of the high expectations about their application areas, especially as antifriction, fire retardant and others materials [1–4]. However, as additives, borate is difficult to dispersions in organic solvent. Researchers found that surface-modified nanoparticles may form relatively stable dispersions in organic solvent and possess a pronounced application in tribological industry and polymer industry [5]. Liu et al. [6] synthesized oleic acid (OA)-modified single crystal barium borate uniform nanorods and found that the modified $BaB_4O_7$ nanorods can improve the load carrying capacity and antiwear properties of the base oil. Chen et al. [7] prepared a new netlike nano size zinc borate by coordination homogeneous precipitation and found that the products had excellent effect on char formation when it was introduced into polypropylene and high-density polyethylene as flame-retardant filler. Qiao [8] synthesized an N-modified nano/micrometer borate by an ultrasonic dispersion and emulsion reaction in the microemulsion phase and found that the modified borate salt revealed an excellent tribological performance. On the other hand, previous investigators suggested that separation of nanoparticles from mother microemulsion solution was difficult [9]. Nowadays, the popular way to synthesize nano-borate is that the borax and OA dissolved into distilled water or absolute ethanol, and the other compound (such as $ZnSO_4$, $BaSO_4$) solution is added to the first solution [10]. The ammonia was added into the solution to control the PH value in the temperature range of 45–80 °C. Furthermore, many researchers tried to synthesis nanoparticles with different morphologies to improve their properties [1, 3, 7, 11, 12].

On the other hand, rare earth materials possess some special properties, such as lanthanum compounds have been evaluated as lubricating oil additives and shown excellent tribological properties [10, 13–16]. Previous investigators suggested that lanthanide complexes are useful anti-abrasion and antiwear additives in oil or grease [10, 13]. Hu et al. [16] synthesized nanoparticles amorphous lanthanum borate with

Z. Jia · Y. Xia (✉)
State Key Laboratory of Solid Lubrication, Lanzhou Institute of Chemical Physics, Chinese Academy of Sciences, Lanzhou 73000, People's Republic of China
e-mail: xiayanqiu@yahoo.com

Z. Jia
College of Materials Science and Engineering, Liaocheng University, Liaocheng 252059, People's Republic of China

a particle size of 20–40 nm and found that the nanoparticles of amorphous lanthanum borate as additives possessed better wear resistance and load carrying capacity than base oil. In this paper, a facile and easy hydrothermal route was reported to synthesize lanthanum borate nanoparticles. Then, the lanthanum borates were capped by OA. And the friction-reducing and anti-wear functions for the steel/steel and steel/laser treated AISI 1045 steel pairs were investigated under PAO containing the three OANLBs. At the same time, the tribological mechanism was also analyzed.

## 2 Experimental Details

In a typically synthesis, 3.8 g borax and 3.0 g $La(NO_3)_3$ was dissolved into 50 and 10 mL distilled water, respectively, with vigorous stirring for 1 h. The $La(NO_3)_3$ solutions were added dropwise into the borax solution with stirring at room temperature, and the precipitate appeared rapidly (code as: S1). The sediment was filtrated and washed repeatedly using distilled water and absolute ethanol, respectively. The filtrated cake and 1.0 mL OA were re-dispersed by ultrasonic into 60 mL *n*-butanol to form homogeneous phase. The homogeneous slurry was transferred into a round-bottom flask and stirred under reflux conditions for 0.5 h. Finally, the *n*-butanol was distilled away under reduced pressure to get the aim compound of OANLB-1. As for OANLB-2, the S1 was sealed in a 100 mL Teflon-lined stainless steel autoclave, and heated at 130 °C for 10 h and then cooled to room temperature. Other steps are as the same as OANLB-1. The difference between OANLB-3 and OANLB-2 is that the ammonia was added into the S1 to maintain the pH at 9.

AISI 1045 steel discs (Ø 24 mm × 7.8 mm) were polished (hardness 230 HV, surface roughness 0.03 μm) before laser quenching the surfaces. The laser quenching was conducted on a 10 kW transverse-flow continuous 4-axis computer numerical controlled (CNC) laser material processing machine tool. The process was executed with a laser beam size of 20 mm × 1 mm, discharge power of 6 kW, velocity of 1000 mm/min. Furthermore, the two-dimensional (2D) and three-dimensional (3D) profiles of the surface were shown in Fig. 1. Commercial PAO (kinetic viscosity at 40 °C: 68 $mm^2/s$) was used as the base oil and the additive content (mass fraction) was fixed at 1.0 wt%. The OANLBs can be dispersed in PAO stably. The friction and wear behavior of AISI 1045 steel and laser treated AISI 1045 steel under the lubrication of pure PAO and PAO containing OANLBs was evaluated using a reciprocating ball-on-disc friction and wear tester. The upper balls with diameter of 10 mm were made of AISI 52100 steel. The lower stationary discs of laser treated AISI 1045 steel (0.42% C, 0.17% Si, 0.5% Mo, 0.035% P, 0.025% Cr, 0.030% Ni, 0.25% Cu, remainder Fe) had a surface roughness (Ra) of 0.03 μm and hardness of 650 HV. The sliding tests were performed at an amplitude of 1 mm, a test duration of 30 min, normal load of 20 N, and reciprocating frequency of 10, 20, 30, 40, and 50 Hz (corresponding maximum sliding speeds are 0.02, 0.04, 0.06, 0.08, and 0.10 m/s), at room temperature. Separate tests were done for each frequency and three repeat measurements were carried out, and the averaged values of the friction coefficients and wear rates are reported in this paper. The FTIR spectrum is recorded in the range of 500–4000 $cm^{-1}$ by Bruck IFs66v spectrometer. Field-emission scanning electron microscopy (FE-SEM) images were obtained on a JEOL JSM-6701SEM. TEM images were obtained on a JEM-1200 EX TEM. X-ray photoelectron spectroscopy (XPS) was performed on a PHI-5702 multi-functional X-ray photoelectron spectroscope to investigate the chemical states of the worn surface. Al Kα radiation was used as the excitation source to determine the binding energies of the target elements at a pass energy of 29.4 eV and a resolution of ±0.2 eV. The binding energy of C1s (284.6 eV)

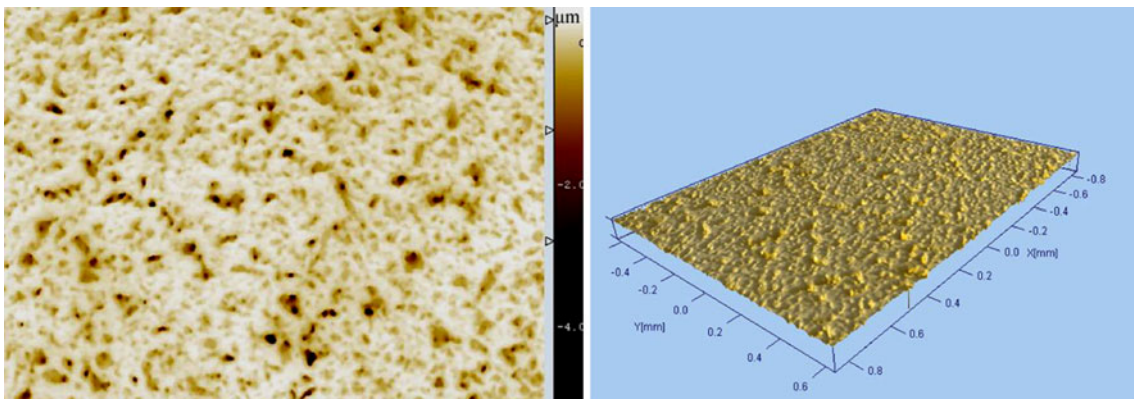


**Fig. 1** The 2D and 3D profiles of the laser quenching surface

was used as the internal reference [17]. The morphologies and elemental composition of the worn surfaces were analyzed using a JSM-6500LV scanning electron microscope equipped with an attachment for energy dispersive X-ray analysis (SEM-EDXA, Kevex Sigma, USA). The thermogravimetry (TG) was carried out on Netzsch STA499 simultaneous thermal analyzer at a heating rate of 10 °C $min^{-1}$ under $N_2$. The wear volume loss of lower disc was determined using a Microxam-three dimensional surface profiler (ADE Corporation of America).

## 3 Results and Discussions

### 3.1 Characterization of Lanthanum Borate

Figure 2 displays the FT-IR spectra of the lanthanum borate and OANLBs. The band at 3404 $cm^{-1}$ is attributed to O–H stretching vibration [6]. The band at 1655 $cm^{-1}$ is attributed to the H–O–H bending mode, which indicates that the compound contains the crystal water [1, 2, 6]. The band at 1390 and 986 $cm^{-1}$ should be the asymmetric and symmetric stretching of B–O band [1, 2]. As for OANLBs, the band at 1548 $cm^{-1}$ is attributed to the existence of carboxylic acid salt in OA-capped lanthanum borate [18]. The band at 2925 and 2853 $cm^{-1}$ is assigned to the stretching vibration of $CH_2$ group [6]. Figure 3 shows the TG analysis results of lanthanum borate and OANLB. Obviously, the weight loss of lanthanum borate is about 15% and that of OANLB is about 35%. So, the conclusion can be easily drawn that the ratio of OA is about 20%.

Figures 4 and 5 show the FE-SEM and TEM images of OANLBs. As for the OANLB-1, the diameter of the nanoparticles was about 10 nm (see Fig. 5a). Comparing OANLB-1, OANLB-2 showed increasing diameter. More interestingly, the leaf-like lanthanum borate appeared as

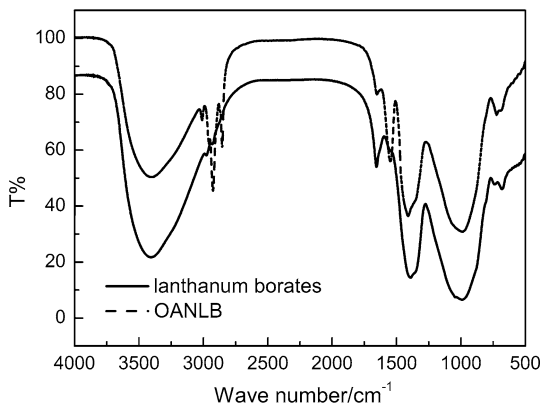


**Fig. 2** FT-IR absorption spectra of unmodified lanthanum borate, and OANLB

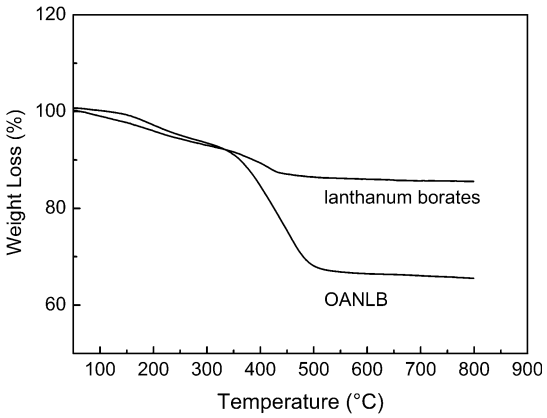


**Fig. 3** TG analysis of unmodified lanthanum borate, and OANLB

the ammonia added into the system (see OANLB-3). The thickness of these leaves was about 5 nm (see Fig. 5c). A slight agglomeration happened when the additives were dispersed into PAO.

### 3.2 Tribological Properties

Figure 6 shows the friction coefficient and wear rate of the steel/steel pair lubricated with the pure PAO and PAO containing OANLBs at 20 N for 30 min. The friction coefficients of the PAO and PAO containing OANLBs are significant different at all frequencies. Namely, the friction coefficient of the AISI 1045 steel lubricated with PAO is much higher than that of PAO containing OANLBs, respectively. At 50 Hz, the friction coefficient of the AISI 1045 steel lubricated with PAO is about 0.37, but that with PAO containing OANLB-1 and OANLB-2 is only 0.13. As for the three OANLBs, the OANLB-1 and OANLB-2 possess better friction-reducing ability than OANLB-3 under all frequencies. At the same time, the volume wear rate of the AISI 1045 steel lubricated with PAO is about five times bigger than that of PAO containing the OANLBs at 10 Hz.

In order to observed influence of modified materials, laser treated AISI 1045 steel was chosen as the low disc. Figure 7a shows the friction coefficients of the steel/laser treated AISI 1045 steel pair lubricated with PAO and PAO containing OANLBs at 20 N. Obviously, the friction coefficients of steel/laser treated AISI 1045 steel pairs lubricated with PAO containing the three OANLBs is smaller and more stable than that of pure PAO under all frequencies. The PAO containing OANLB-2 has the smallest friction coefficient in the all frequencies, and the friction coefficient is only 0.09. At 50 Hz, the friction coefficient of pure PAO is 0.21. The various wear rates of laser treated AISI 1045 steel lubricated with PAO and PAO containing OANLBs at different frequencies are shown in Fig. 7b. The laser treated disc obviously has a better wear resistance when lubricated

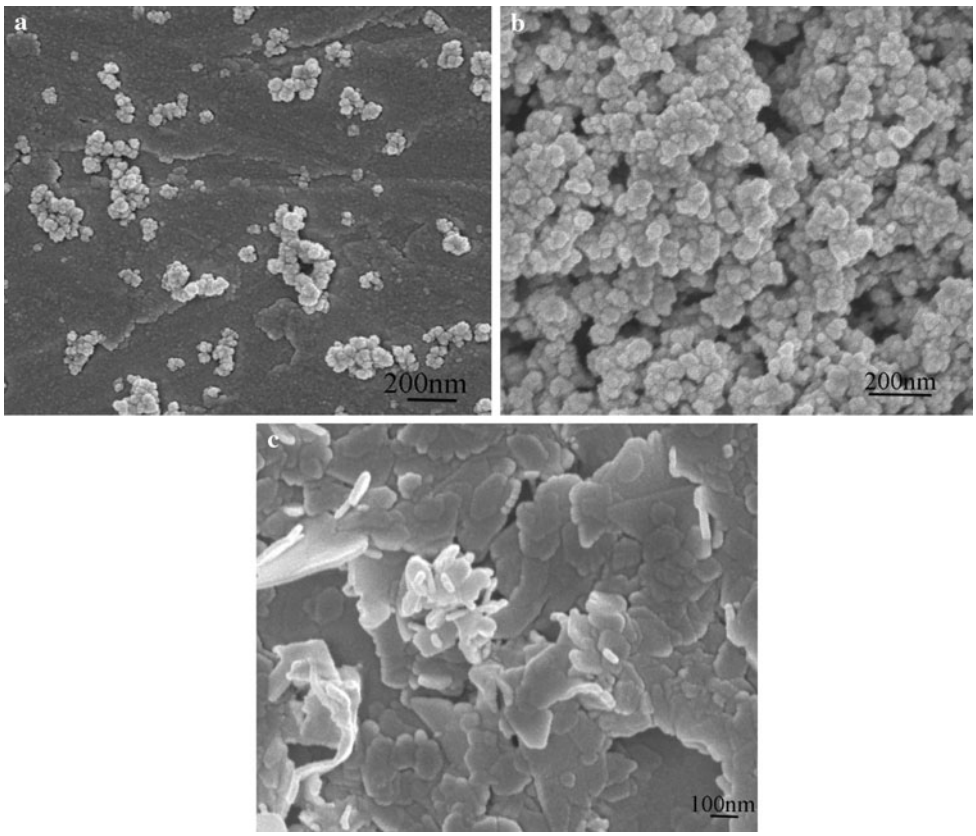


**Fig. 4** FE-SEM imagines of OANLB-1 (**a**), OANLB-2 (**b**), and OANLB-3 (**c**)

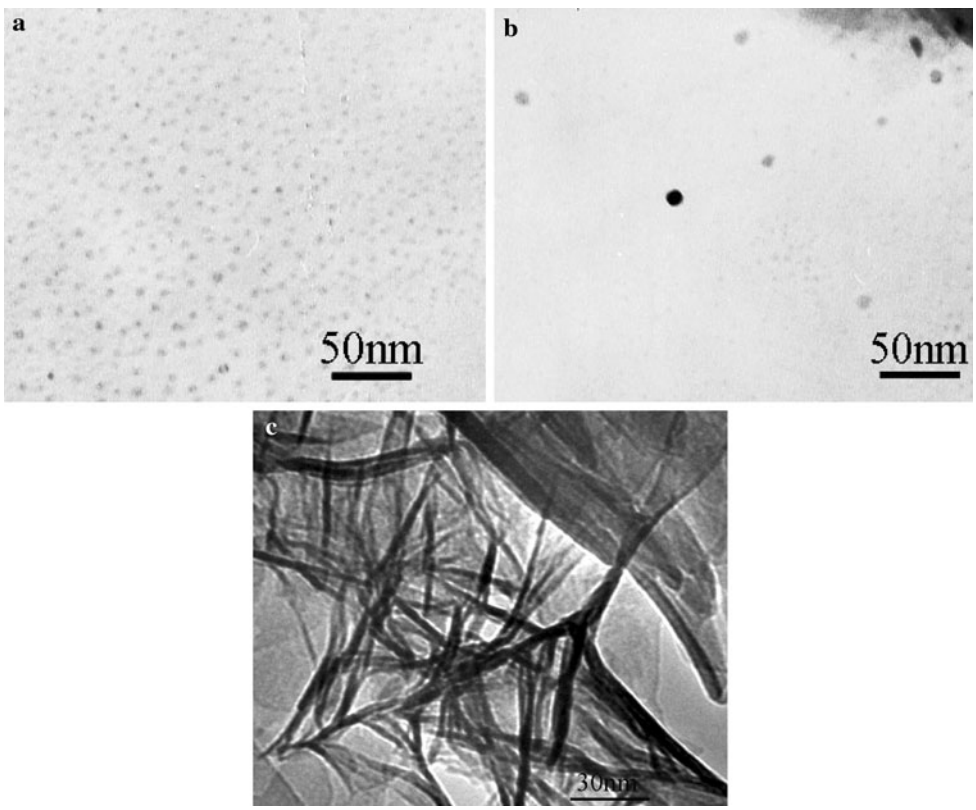


**Fig. 5** TEM imagines of OANLB-1 (**a**), OANLB-2 (**b**), and OANLB-3 (**c**)

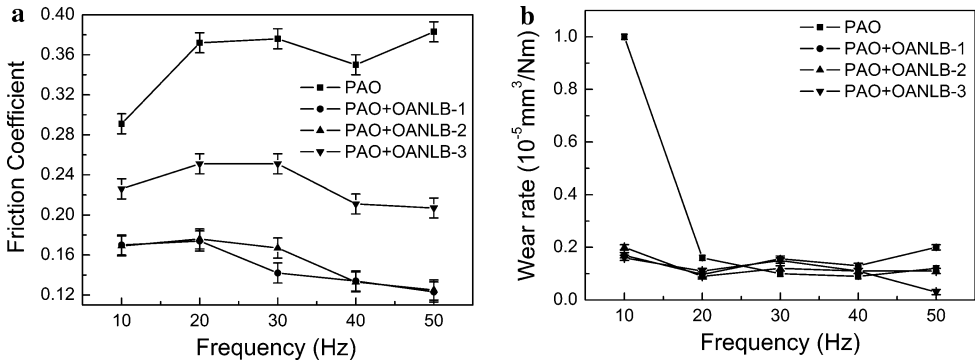


**Fig. 6** Friction coefficients (**a**) and wear rates (**b**) of the steel/steel pair lubricated with PAO and PAO containing OANLBs (20 N, 30 min)

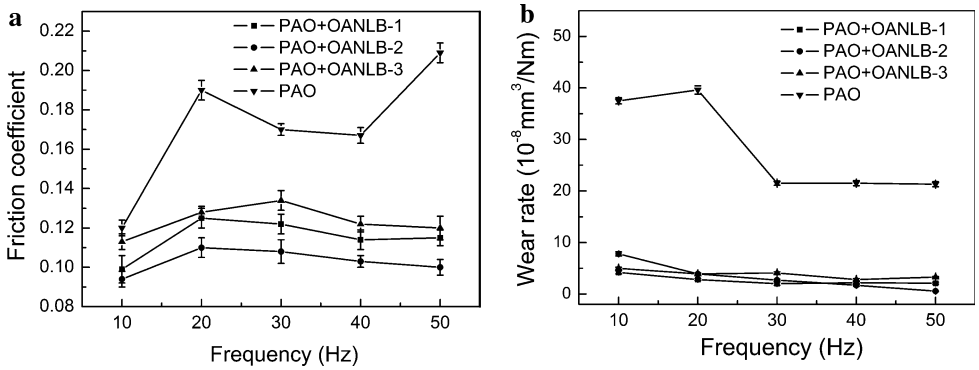


**Fig. 7** Tribological performance of steel/laser treated AISI 1045 steel contact in combination with the PAO and PAO containing OANLBs, **a** friction coefficient curves, **b** wear rate curves (20 N, 30 min)

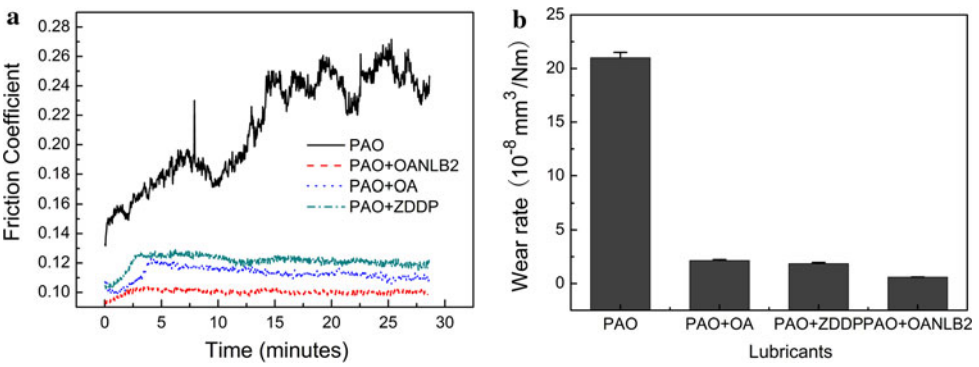


**Fig. 8** Friction coefficient line (**a**) and wear rate (**b**) of the PAO, PAO + OA, PAO + OANLB2, and PAO + ZDDP at 50 Hz for 30 min

with PAO containing the OANLBs than that with pure PAO. More interestingly, the wear rate of laser treated AISI 1045 steel lubricated with the PAO containing OANLBs is constant at $3.5 \times 10^{-8}$mm$^3$/Nm in all frequencies, which is approximately 5–10 times lower than that of pure PAO in the whole frequency range.

Comparing the Figs. 6a and 7a, the friction coefficients of the laser treated AISI 1045 steel lubricated with PAO and PAO containing OANLBs are smaller than that of the AISI 1045 steel. At 50 Hz, the friction coefficient of laser treated AISI 1045 steel lubricated with PAO containing OANLB-3 is about 0.12, but that of AISI 1045 steel is about 0.22. Furthermore, the wear rate of the laser treated AISI 1045 steel lubricated with the PAO and PAO containing OANLBs is significant smaller than that of the AISI 1045 steel in all frequencies (as shown in Figs. 6b and 7b). Comparing the AISI 1045 steel and laser treated AISI 1045 steel, the surface hardness of the sample increased from 230 to 650 HV. It is reasonable to deduct that laser quenching coatings plays an important role on anti-wear and friction-reducing. Figure 8 shows the friction coefficient and wear rate of PAO and PAO containing OA, ZDDP, and OANLB2, respectively, at 50 Hz for 30 min. Obviously, the friction coefficient of PAO is the highest among the four lubricants. On the other hand, the friction coefficient of PAO containing OANLB2 is the lowest. As for the wear rate of the four lubricants, the wear rate of PAO is much higher than that of other three lubricants.

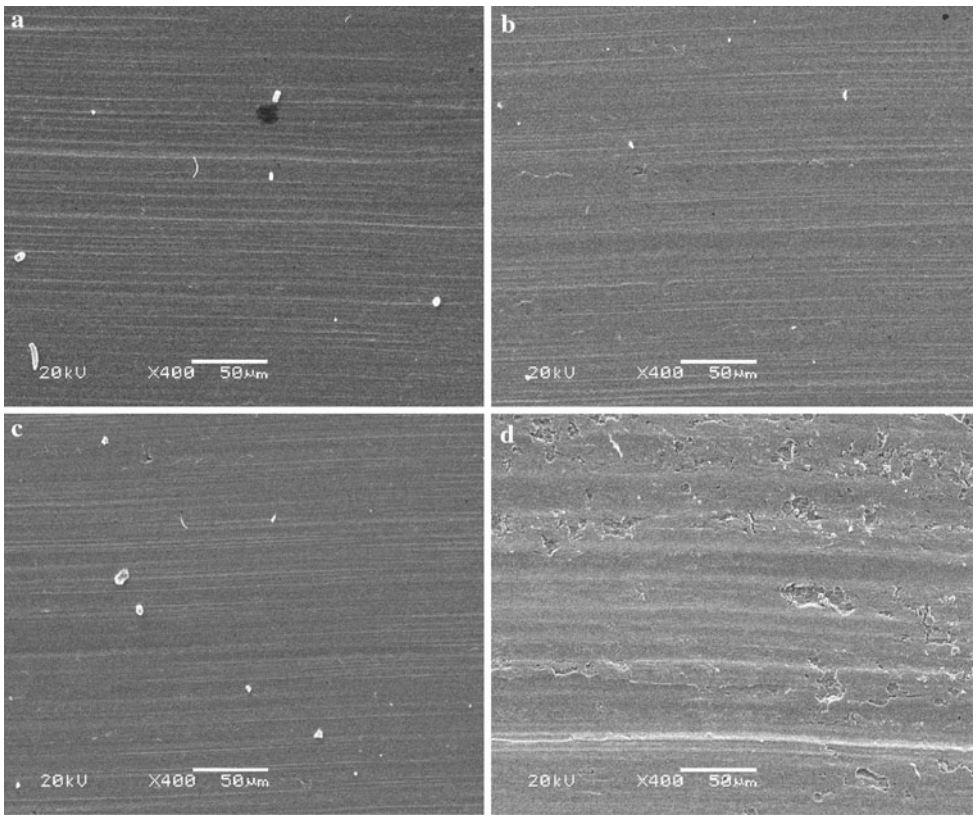


**Fig. 9** SEM photographs of worn surfaces of AISI 1045 steel lubricated with **a** PAO + OANLB-1, **b** PAO + OANLB-2, **c** PAO + OANLB-3, **d** PAO

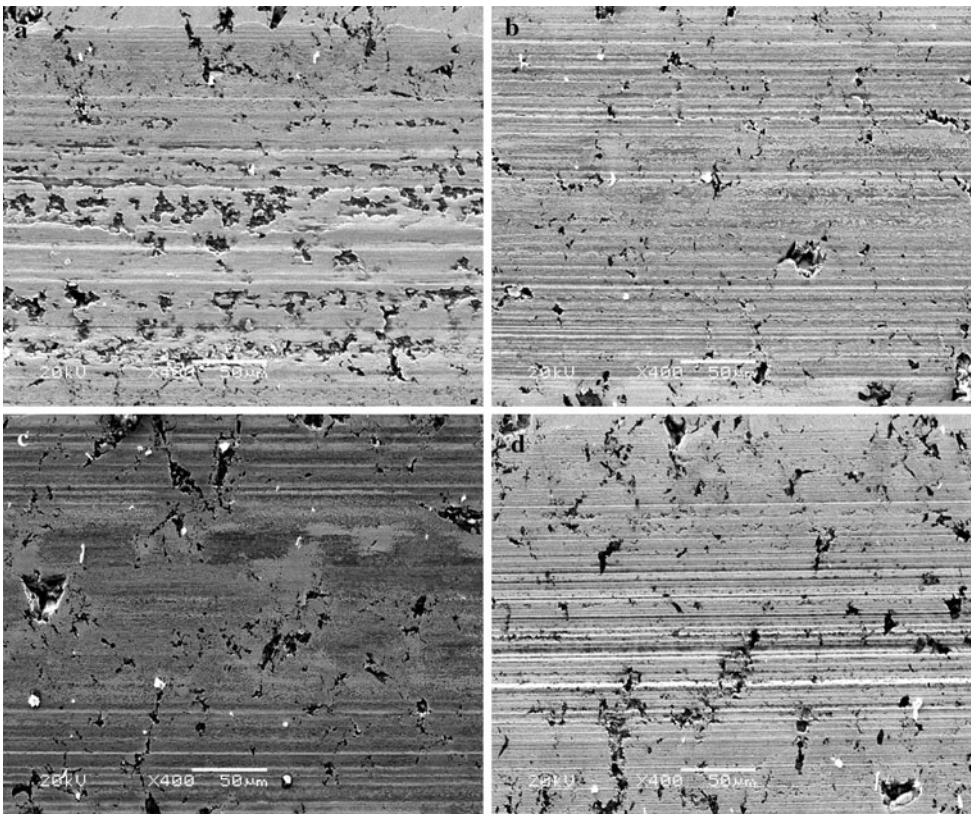


**Fig. 10** SEM photographs of worn surfaces of laser treated AISI 1045 steel lubricated with **a** PAO + OANLB-1, **b** PAO + OANLB-2, **c** PAO + OANLB-3, **d** PAO

Furthermore, the wear rate of PAO containing OANLB2 is only $0.6 \times 10^{-8}$mm$^3$/Nm, which is the lowest among the four lubricants.

### 3.3 SEM and XPS Analyses of Worn Surfaces

In order to investigate the friction-reducing and anti-wear properties of the PAO and PAO containing OANLBs for the two kinds of sliding pairs, the worn surfaces of AISI 1045 steel and laser treated AISI 1045 steel were ultrasonically washed with acetone and analyzed using SEM. As for the steel/steel pair, the worn surfaces of the AISI 1045 steel under the lubrication of the PAO containing the three OANLBs are smoother and show slighter adhesion as compared with that of the pure PAO under the same condition (see Fig. 9a–d). Possibly, the tribofilm protected the worn surface during sliding.

Figure 10 shows the SEM photographs of the worn surface of the laser treated AISI 1045 steel lubricated with the PAO and PAO containing OANLBs at a load of 20 N for 30 min. Obviously, the worn surface of the laser treated specimen lubricated with PAO showed more severe adhesion wear than that of lubricated with PAO containing OANLBs. Namely, the worn surface of the laser treated AISI 1045 steel lubricated with PAO showed a deeper plough than that with PAO containing OANLBs (see

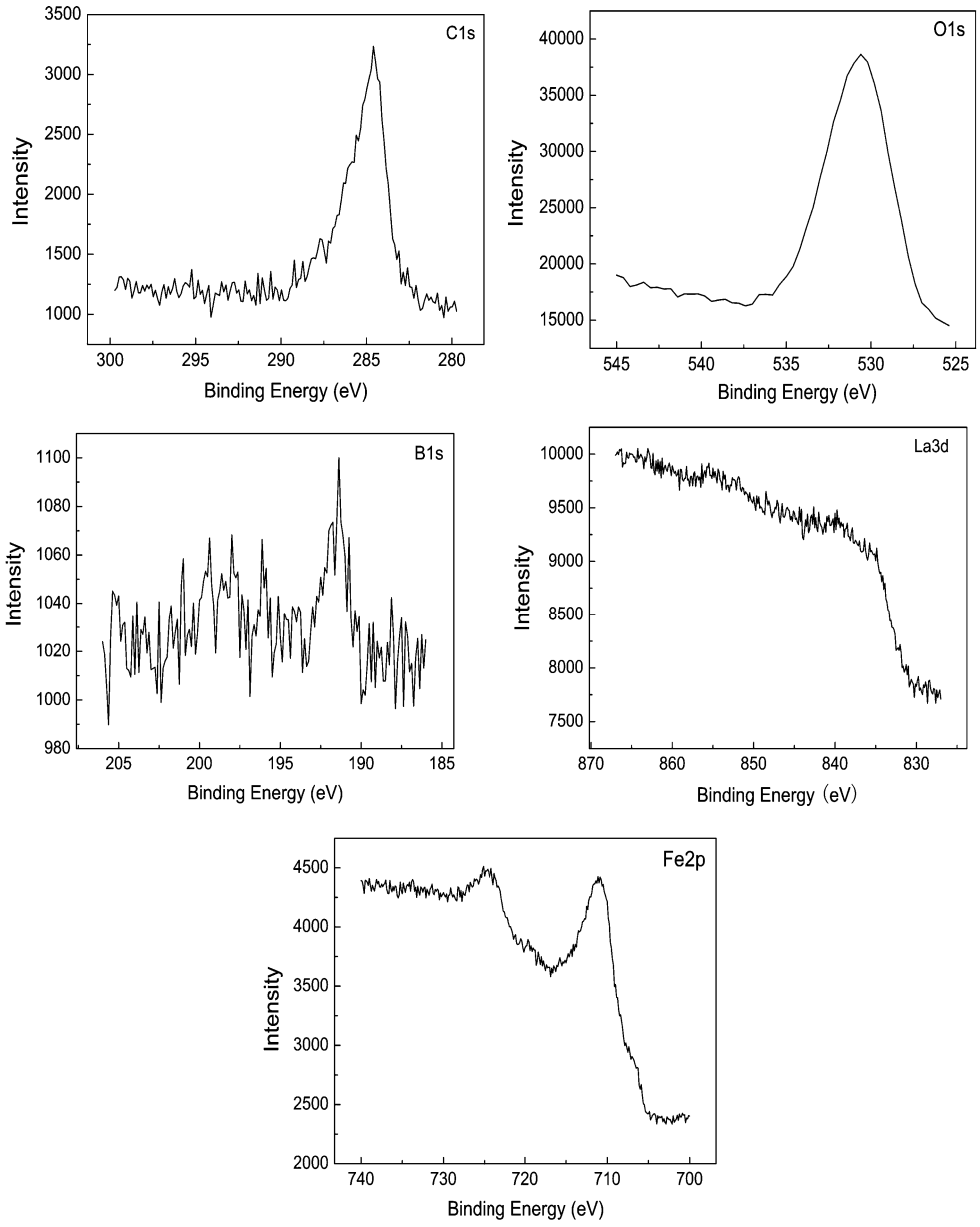


**Fig. 11** XPS spectra of several elements on the worn surface of the laser treated AISI 1045 steel lubricated with PAO + OANLB-1 (20 N, 50 Hz, 30 min)

Fig. 10d and a, b, c), which well corresponds to the wear rate of the laser treated AISI 1045 steel (see Fig. 7).

The worn surfaces of the steel/laser treated AISI 1045 steel pairs lubricated with the PAO containing OANLBs were analyzed by mean of XPS so as to acquire more information about the tribochemical reactions involved during the sliding process. Figure 11 shows the XPS spectra of C1s, O1s, B1s, La3d, and Fe2p on the worn surface of laser treated AISI 1045 steel lubricated with PAO containing OANLB-1. The broad peak of B1s from 191.0 to 192.3 eV is attributed to $B_2O_3$ [19–21]. Fe2p peak from 710.0 to 712.0 eV might be assigned to $Fe_2O_3$ on the worn surface [20]. But, unfortunately, the peak of La3d is very weak. The XPS spectra of the B1s, La3d, and Fe2p on the worn surface of the upper ball lubricated with PAO containing OANLB-1 are shown in Fig. 12. The broad peak of Fe2p from 709.9 to 712.0 eV might indicate the $Fe_2O_3$ on the worn surface [20]. The spectrum of La3d centered at 835.2 eV is attributed to $La_2O_3$ [15, 17]. The broad peak of B1s centered at 191.3 eV is assigned to $B_2O_3$ [16, 21]. On the other hand, the spectra of B1s and La3d are very weak, possibly because the tribofilm on the upper ball is too slight to be detected. The peak of B1s at 197.3 eV is might attributed to the existence of La4p3/2 on the worn surface [17]. It is reasonable to conclude that the tribofilm containing La, B, and Fe formed during sliding, which

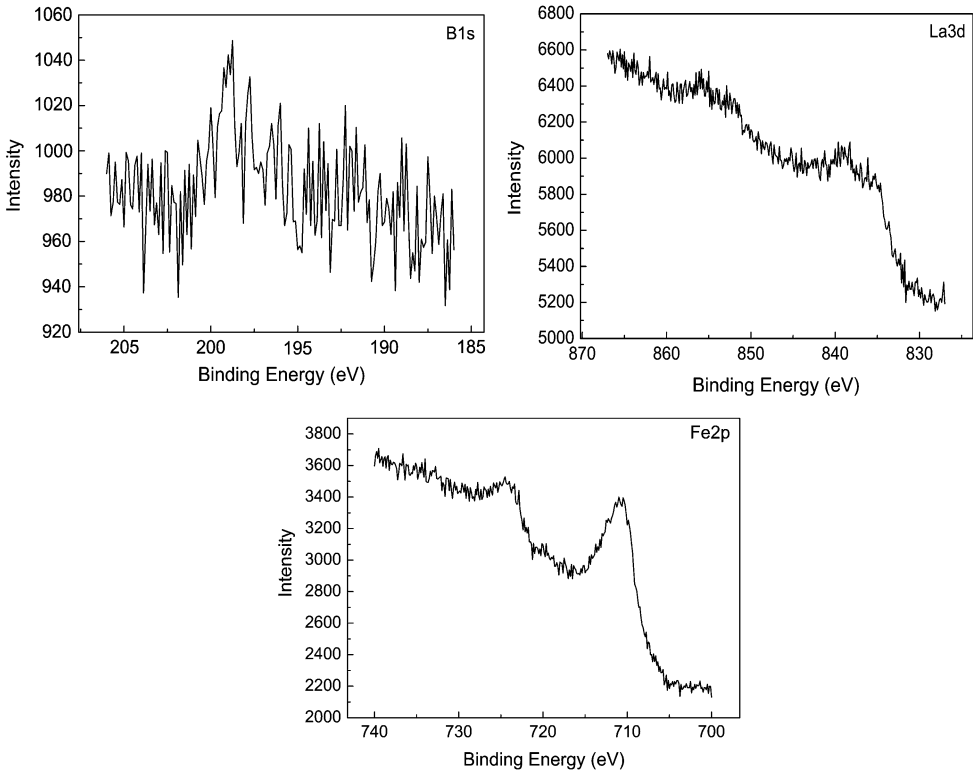


**Fig. 12** XPS spectra of several elements on the worn surface of the upper ball of the steel laser treated AISI 1045 steel pairs lubricated with PAO + OANLB-1 (20 N, 50 Hz, 30 min)

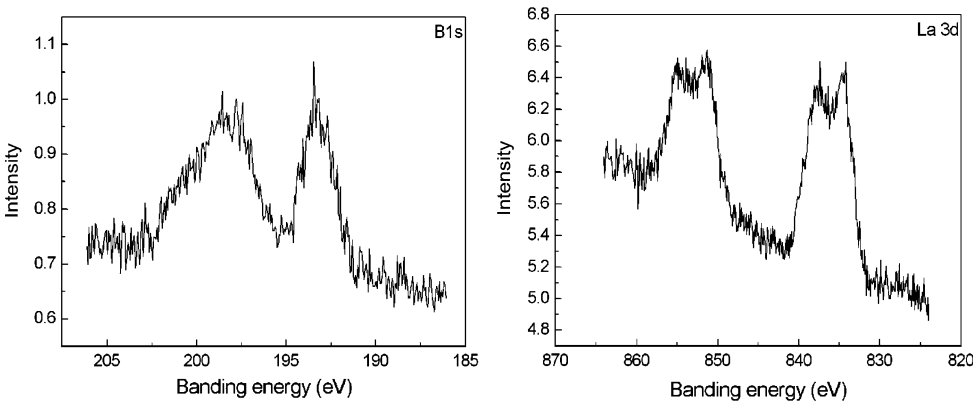


**Fig. 13** XPS spectra of lanthanum borate

improved the wear resistance of the steel/laser treated AISI 1045 steel pairs.

## 4 Discussion

Although the chemical interaction between lubricants and worn surface is too complicated to be disclosed satisfactorily, we try to find some clues of the mechanism. Figure 13 shows the XPS analysis of the lanthanum borate powder. Obviously, the peak at about 193.2 eV of B1s is attributed to $B_2O_3$ [19–21]. On the other hand, the broad peak of B1s from 197.4 to 198.8 eV possibly can be considered La4p3/2, and the existence of La is reasonable to be deducted [17]. The broad peak of La3d from 834.1 to 835.7 eV shows the existence of $La_2O_3$ [15]. So, it is reasonable to presume that the nano lanthanum borates are composed of $B_2O_3$ and $La_2O_3$, lubricating the steel/laser treated AISI 1045 steel pair during sliding because of their special structure. It is reasonable to deduct that the OANLBs was discomposed into $La_2O_3$ and $B_2O_3$ during sliding, and both of them improved the tribological properties of laser treated AISI 1045 steel. On the other hand, the EDS analysis was executed to get more information of the worn surface (see Table 1). Obviously, the atomic percentage of La is 0.2 after sliding, but, that is 0.00 after washing. It is reasonable to conclude that $La_2O_3$ was washed away by acetone (shown as Fig. 14). Furthermore, the atom of B can be penetrated into the sublayer of the worn surface because of its small diameter [19–21], which is corresponding to the high percentage of B (shown in Table 1). It is more reasonable to understanding that the tribofilm of the worn surface of laser treated AISI 1045 steel was composed of B, Fe and La, although the La was very weak after sliding [16].

**Table 1** The EDS analysis of the OANLB and worn surface

| Sample | C (at.%) | O (at.%) | B (at.%) | La (at.%) | Fe (at.%) |
|---|---|---|---|---|---|
| OANLB2 | 53.25 | 2.43 | 8.96 | 34.21 | 1.16 |
| After sliding | 46.73 | 0.98 | 24.16 | 0.2 | 27.94 |
| After washing | 37.2 | 0.68 | 21.72 | 0.00 | 40.40 |

## 5 Conclusions

Following conclusions can be drawn from above results:

OANLBs were synthesized by an eco-friendly hydrothermal method; the morphologies of these particles can be controlled with a facile and easy way. Namely, the diameters of these particles increased under high temperature and high pressure, the morphology of these particles changed into leaf under high PH values.

The laser treated AISI 1045 steel discs showed better tribological properties than that of pure PAO under the lubrication of PAO containing OANLBs. At 50 Hz, the friction coefficients of steel/laser treated AISI 1045 steel pair lubricated with PAO containing OANLBs is not more than 0.12, but that with pure PAO is 0.21. Moreover, the wear rate of PAO is about one order of magnitude bigger than that of the PAO containing lanthanum borates at 20 Hz. On the other hand, the wear rate of laser treated AISI 1045 steel discs is approximately three orders of magnitude lower than that of steel discs under lubrication of PAO.

XPS spectra showed that the tribofilm containing B, La, and Fe was formed on the worn surfaces of the laser treated AISI 1045 steel discs under the lubrication of the PAO containing the three OANLBs. The resulting surface protective films together with laser treated AISI 1045 steel surface contributed to significantly reduce the friction and wear.

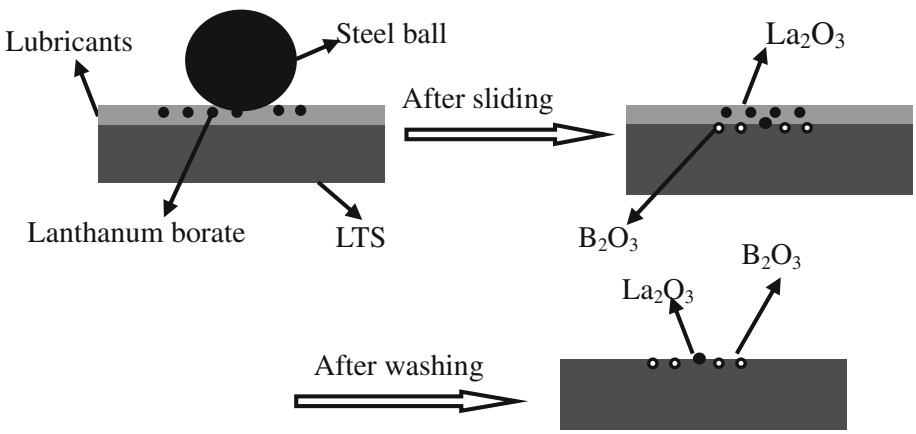


**Fig. 14** Schematic diagram of wear resistance mechanism of the lanthanum borate

**Acknowledgments** The authors would like to thank the financial support of this work by "Hundred Talents Program" of CAS, Natural Science Foundation of China (Grant No.50905177), and "973" program (2007CB607606).

## References

1. Chen, T., Deng, J.C., Wang, L.S., Feng, G.: Preparation and characterization of nano-zinc borate by a new method. Mater Process Technol **209**, 4076–4079 (2009)
2. Tian, Y.M., Guo, Y.P., Jiang, M., Sheng, Y., Hari, B., Zhang, G.Y., et al.: Synthesis of hydrophobic zinc borate nanodiscs for lubrication. Mater Lett **60**, 2511–2515 (2006)
3. Shi, X.X., Xiao, Y., Yuan, L.J., Sun, J.T.: Hydrothermal synthesis and characterizations of 2D and 3D $4ZnO{\cdot}B_2O_3{\cdot}H_2O$ nano/microstructures with different morphologies. Powder Technol **189**, 462–465 (2009)
4. Zhou, J., Su, D.G., Luo, J.M., Zhong, M.F.: Synthesis of aluminum borate nanorods by a low-heating-temperature solid-state precursor method. Mater Res Bull **44**, 224–226 (2009)
5. Bakunin, V.N., Suslov, A.Y., Kuzmina, G.N., Parenago, O.P.: Recent achievements in the synthesis and application of inorganic nanoparticles as lubricants components. Lubr Sci **17**, 127–145 (2005)
6. Liu, N., Tian, Y.M., Yu, L.X., Li, Q.J., Meng, F.Y., Zheng, Y.H.: Synthesis and surface modification of uniform barium borate nanorods for lubrication. J Alloys Compd **466**, L11–L14 (2008)
7. Chen, T., Deng, J.C., Wang, L.S., Fan, Y., Gang, F.: Synthesis of a new netlike nano zinc borate. Mater Lett **62**, 2057–2059 (2008)
8. Qiao, Y.L., Liu, W.M., Xu, B.S., Ma, S.N., Xue, Q.J.: The tribochemical performance of nano/micrometer borate modified by an N-containing compound as an oil additive. Lubr Sci **15**, 369–379 (2003)
9. Bonini, M., Bardi, U., Berti, D., Neto, C., Baglioni, P.: A new way to prepare nanostructured materials: flame spraying of microemulsions. J Phys Chem B **106**, 6178–6183 (2002)
10. Liu, W.M., Zhang, Z.F., Xue, Q.J.: Friction and wear behaviors of aluminum-on-steel under the lubrication of grease containing a complex of lanthanum dialkyldithiocarbamate and phenanthroline. Wear **199**, 153–156 (1990)
11. Standnes, H.: Analysis of oil recovery rates for spontaneous imbibition of aqueous surfactant solutions into preferential oil-wet carbonates by estimation of capillary diffusivity coefficients. Colloids Surf A **251**, 93–101 (2004)
12. Olson, W.D., Muir, R.J., Eliades, T.I., Steib, T.: Improved sulfonate greases. EP 0613940A2 (1994)
13. Liu, W.M., Gao, C.Z., Zhang, Z.F., Xue, Q.J.: Tribological properties of aluminum-on-steel system under the lubrication of grease containing a complex of lanthanum N-salicylidene derivative of malonic dihydrazide. Wear **196**, 234–237 (1996)
14. Zhang, Z.F., Liu, W.M., Xue, Q.J.: Study on lubricating mechanisms of $La(OH)_3$ nanocluster modified by compound containing nitrogen in liquid paraffin. Wear **218**, 139–144 (1998)
15. Zhang, Z.F., Liu, W.M., Xue, Q.J.: The tribological behaviors of succinimide-modified lanthanum hydroxide nanoparticles blended with zinc dialkyldithiophosphate as additives in liquid paraffin. Wear **248**, 48–54 (2001)
16. Hu, Z.S., Dong, J.X., Chen, G.X., He, J.Z.: Preparation and tribological properties of nanoparticle lanthanum borate. Wear **243**, 43–47 (2000)
17. Moulder, J.F., Stickle, W.F., Sobol, P.E., Bomben, K.D.: Handbook of X-ray Photoelectron Spectroscopy. Physical Electronics, Inc Press, Eden Prairie (1995)
18. Chen, S., Liu, W.M.: Oleic acid capped PbS nanoparticles: synthesis, characterization and tribological properties. Mater Chem Phys **98**, 183–189 (2006)
19. Jia, Z.F., Wang, P., Xia, Y.Q., Zhang, H.B., Pang, X.J., Li, B.: Tribological behaviors of diamond-like carbon coatings on plasma nitrided steel using three BN-containing lubricants. Appl Surf Sci **255**, 6666–6674 (2009)
20. Jia, Z.F., Xia, Y.Q., Li, J.L., Pang, X.J., Shao, X.: Friction and wear behavior of diamond-like carbon coating on plasma nitrided mild steel under boundary lubrication. Tribol Int **43**, 474–482 (2010)
21. Zheng, Z., Shen, G.Q., Wan, Y., Cao, L.L., Xu, X.D., Yue, Q.X., Sun, T.J.: Synthesis, hydrolytic stability and tribological properties of novel borate esters containing nitrogen as lubricant additives. Wear **222**, 135–144 (1998)